RESEARCH ARTICLE

Temporal shifts of the Norway lobster (*Nephrops norvegicus*) gut bacterial communities

Alexandra Meziti[1,2], Alban Ramette[2], Eleni Mente[1,3] & Konstantinos Ar. Kormas[1]

[1]Department of Ichthyology and Aquatic Environment, University of Thessaly, Magnisia, Greece; [2]Max Planck Institute for Marine Microbiology, Bremen, Germany; and [3]School of Biological Sciences, University of Aberdeen, Aberdeen, Scotland, UK

Correspondence: Konstantinos Ar. Kormas, Department of Ichthyology and Aquatic Environment, University of Thessaly, 384 46 Nea Ionia, Magnisia, Greece.
Tel.: +30 242 109 3082; fax: +30 242 109 3157; e-mail: kkormas@uth.gr

Received 7 March 2010; revised 20 July 2010; accepted 30 July 2010.
Final version published online 10 September 2010.

DOI:10.1111/j.1574-6941.2010.00964.x

Editor: Julian Marchesi

Keywords
Bacteria; FISH; ARISA; 16S rRNA gene; gut; *Nephrops norvegicus*.

Abstract

The aim of this study was to investigate the gut bacterial communities of *Nephrops norvegicus* individuals, using a suite of molecular tools consisting of automated ribosomal intergenic spacer analysis, 16S rRNA gene–internal transcribed spacer clone libraries and FISH. The animals were collected from Pagasitikos Gulf, Greece, during different months of the year. The diversity of the gut bacterial communities was found to mostly vary with sampling time, which could be related to temporal variations in food supply. The 16S rRNA gene diversity analysis showed dominance of specific phylotypes for each month studied. February, May, July, August and October samples were rich in sequences related to the gammaproteobacterial genera *Pseudoalteromonas*, *Psychrobacter* and *Photobacterium*. September and December samples were dominated by phylotypes affiliated with uncultured representatives of *Mollicutes*, which are generally associated with the intestinal tracts of various animals. The presence of *Gammaproteobacteria* and uncultured *Mollicutes* in August and September samples, respectively, was further confirmed by FISH. None of the morphometric parameters considered was related to the temporal pattern of dominant bacterial communities.

Introduction

The Norway lobster *Nephrops norvegicus* (also called Dublin bay prawn) is a burrowing decapod crustacean living at 20–800 m depth. It is widely distributed on muddy substrata throughout the northeast Atlantic Ocean from Iceland in the north to Morocco in the south, at the British coasts and in the Mediterranean Sea and has a high commercial importance in these areas (Bell, 2009). However, concerns about possible depletion and recruitment failure for *Nephrops* fisheries have been expressed due to overexploitation and insufficient or inappropriate management strategies. *Nephrops norvegicus* feeds mainly on fish, molluscs, crustaceans, polychaetes, echinoderms and foraminifera (Cristo & Cartes, 1998). Differences in diet are attributed mainly to differences in prey abundance rather than to differences in prey preference. *Nephrops norvegicus* is considered to be an opportunistic predator and a scavenger. It has been suggested that it can act as a suspension feeder. This occurs when food resources are limited (Loo *et al.*, 1993). In captivity, cannibalism has also been observed when food supply is insufficient (Sarda & Valladares, 1990) and when other individuals are vulnerable, for example due to molting (A. Meziti, I. Karapanagiotidis, K. Kormas & E. Mente, pers. commun.).

The digestive system of *N. norvegicus* consists of three parts: (1) the foregut, consisting of the esophagus, the cardiac and the pyloric stomach, (2) the midgut, which includes the hepatopancreas and the intestine till the sixth abdominal segment and (3) the hindgut, which is the last very short chitin-lined part after the midgut leading to the anus. The main part of the food assimilation occurs in the upper part of the midgut either by enzymes excreted from the hepatopancreas or by mechanical disruption from the gastric mill. The midgut is the main absorbing organ, and no absorption occurs in the short hindgut (Yonge, 1924).

Gut microorganisms are considered very important for the nutrition of many animal species including crustaceans (Harris, 1993). The microorganisms grow in a stable environment inside the animal gut, while the host usually benefits either from microbially mediated digestion of ingested food or from important nutrients. However, the microbial

colonization of *N. norvegicus* has not been studied in detail as yet.

Most of the available studies have focused on the hindgut microbiota of other *Decapoda*, mainly *Thalassinidae*, and have found thriving microbial communities because no assimilation of nutrients occurs there and consequently no competition with the hosts (Lau *et al.*, 2002 and references therein). However, over the last years, there has been an increasing interest on the shifts of gut microbial communities driven by the nutritional habits of the host (Ley *et al.*, 2008), making the parts of the intestinal tract where nutrient absorption takes place, such as the *Decapoda* midgut, appropriate systems for the investigation of microorganism–host interactions.

Pagasitikos Gulf, Greece, is a major *N. norvegicus* fishing ground. According to models constructed by Petihakis *et al.* (2005), the sediment surface of the central-external area < 50 m depth is characterized by rather constantly low temperatures (13 °C average) and dim light conditions. Other factors influencing the benthic communities, such as settling phytoplankton biomass, detritus and bacteria, show annual patterns (Petihakis *et al.*, 2005) and are regulated by the phytoplankton bloom starting between January and February each year. Phytoplankton biomass reaches its maximum near the sediment soon after the bloom initiation. Maximum detritus concentrations reach the sediment surface during February and March, causing an almost immediate bacterial response (i.e. increased abundance). After April, a decrease is observed for phytoplankton, detritus and bacterial biomass (Petihakis *et al.*, 2005). These patterns have positive effects on the benthic food web by increasing the activity of suspension and deposit feeders soon after the peaks of phytoplankton, bacteria and detritus around April or May.

The aim of this study was to investigate whether temporal changes, which reflect different food supply, as discussed above, influence the gut microbial communities along with other morphological factors. For this purpose, midgut samples from *N. norvegicus* individuals were collected during different months from the same habitat and were investigated by 16S rRNA gene diversity and internal transcribed spacer (ITS) analysis. To the knowledge of the authors, there is no similar study for the molecular analysis of the gut microbial communities in *N. norvegicus*. Midgut was selected for analysis as the gut part where additional nutrient absorption from the host could occur and a relationship of mutualism with the bacteria could evolve. The examination of the gut bacterial communities provides useful insights into the feeding and nutritional behavior of the animal, especially in commercial rearing efforts that are suggested as alternative to the overexploitation and insufficient or inappropriate management strategies of *N. norvegicus*.

Materials and methods

Nephrops norvegicus collection and morphometric analysis

Samples were collected from Pagasitikos Gulf (Greece) from an area determined by four points: North (39°17.34′N, 23°02.27′E), West (39°15.55′N, 22°56.45′E), South (39°10.33′N, 23°00.59′E) and East (39°09.14′N, 23°08.52′E). Samples were collected monthly in 2007, apart from January, April, June and November, when sampling was not possible due to bad weather conditions or fishing restrictions. Individual, large traps (60 cm × 45 cm × 30 cm) were used to avoid stress on the animals during capture. The traps were left at the bottom of the sea for a maximum of 7 h before retrieving them. Only live animals upon retrieval of the traps were kept for the current work until return to the laboratory ($\leq$ 2 h). The sampling depth varied from 60 to 88 m. After collection, the *N. norvegicus* individuals were immediately transferred on ice to the laboratory, and animal sex, weight, carapace length and width and abdominal width were measured (Supporting Information, Table S1). In total, 53 gut samples were collected for further analysis. Encoding of the samples according to collection month is shown in Table S2.

Midgut isolation

The animals were dissected using sterile lancets and the midgut was extracted using sterile forceps. In order to exclude as many as possible transient bacterial cells ingested with food particles, the extracted midgut was emptied by applying mechanical force and by rinsing in autoclaved particle-free sea water (filtered by 0.2-μm pore size). All dissecting tools were alcohol flame sterilized between each individual sample.

DNA extraction and tissue fixation

DNA extraction was performed on 49 gut tissues from all sampling months using the QIAamp DNA Mini Kit (Qiagen Inc.) following the manufacturer's standard protocol. Some of the gut tissues deriving from the same collection month and from animals of the same sex were pooled for the DNA extraction due to low tissue mass (Table S1). At the final step, DNA was diluted in 100 μL of elution buffer, provided with the kit, and was stored at −20 °C. Because of low numbers of animals available, only samples from August and September were fixed in 4% formaldehyde in sterile 1 × phosphate-buffered saline (PBS) (137 mM NaCl, 2.7 mM KCl, 10 mM Na_2HPO_4, 2 mM KH_2PO_4) at 4 °C for 3 h. Samples were rinsed three times in 1 × PBS for 10 min and were washed in sterile double-distilled water. Samples were stored in 1.5 mL 1 × PBS : ethanol (1 : 1). In total, 39

DNA samples were further analyzed as a result of the pooled tissues and four gut tissues were used for FISH.

Automated ribosomal intergenic spacer analysis (ARISA), nonmetric multidimensional scaling (NMDS) analysis and environmental interpretation

The gut bacterial community structure was estimated by ARISA (Fisher & Triplett, 1999). PCR amplification was conducted in triplicates using primers ITSF (5′-GTCGTAA CAAGGTAGCCGTA-3′) and ITSReub (5′-GCCAAGG CATCCACC-3′) (Cardinale *et al.*, 2004). Primer ITSF was labeled with FAM fluorochrome at the 5′ end. The PCR conditions consisted of an initial denaturation step at 94 °C for 3 min, followed by 30 cycles of 94 °C for 45 s, 55 °C for 45 s, 72 °C for 90 s and a final extension at 72 °C for 5 min. PCR-amplified fragments were purified with Sephadex G-50 Superfine (Sigma-Aldrich, Germany) and the preparation for capillary electrophoresis separation was performed as described previously (Boer *et al.*, 2009). ARISA profiles were analyzed using the GENEMAPPER software v 3.7 (Applied Biosystems Inc., Carlsbad, CA). The total peak area per sample was normalized to one, and only fragments above a threshold of 50 fluorescence units and between 100 and 1000 bp length were considered. GENEMAPPER output files were further analyzed by custom R scripts (Ramette, 2009). To account for size calling imprecision, samples were binned with automatic and interactive binner as described previously (Ramette, 2009). A 'window' of 2.5 bp was selected as the frame offering the highest pairwise similarities among samples and was further subjected to multivariate analyses.

Triplicate profiles were merged to only keep bands that appeared at least twice among the replicates of a given sample (Boer *et al.*, 2009; Ramette, 2009). Unconstrained ordinations were performed to graphically illustrate the relationships between different samples using three-dimensional NMDS (Kruskal, 1964), implemented in R (version 2.7.0). NMDS ordination attempts to place all samples in a three-dimensional space such that their ordering relationships (here based on a Bray–Curtis similarity matrix) are preserved. Hence, the closer the samples are in the resulting ordination, the more similar their overall gut bacterial communities are. Kruskal's stress value reflects the difficulty involved in fitting the samples' relationships into a three-dimensional ordination space. To determine whether season and morphometric data could significantly explain the variation in bacterial community structure, a redundancy analysis (RDA) [reviewed in Ramette (2007)] was implemented in R and its significance was assessed by 999 permutation tests. The *a priori* hypothesis that gut microbial communities differ between different seasons was tested using RDA and the nonparametric ANOSIM (Clarke & Green, 1988). ANOSIM generates a test statistic, R, that ranges from -1 to 1. The magnitude of R is indicative of the degree of separation between groups, with a score of 1 indicating complete separation and 0 indicating no separation (Clarke, 1993). R is unlikely to be substantially smaller than 0 because this would indicate that similarities within groups are systematically lower than those among groups. The critical significance level used for ANOSIM results was $P = 0.05$. Since multiple pairwise comparisons (21) were performed, the Bonferroni correction was applied, decreasing the critical significance level to 0.0024 (0.05/21). It has to be mentioned that the Bonferroni correction has often been judged to be overly conservative (Legendre & Legendre, 1998), and so care should be taken when applied to ecological data. Only results from the ANOSIM method are presented because both methods gave the same conclusions.

Cloning and sequencing of 16S rRNA genes and ITS

Bacterial 16S rRNA gene and the ITS were amplified from samples F1, My46, Jl1, Ag31, Se3, O2 and D1 using the 27f BAC (5′-AGAGTTTGATCMTGGTCAG-3′) (Lane, 1991) and ITSReub primers. Expected amplicon sizes varied from 1800 to 2400 bp due to variation in ITS size. PCR conditions were 2 min at 94 °C, followed by 10 cycles with 30 s at 94 °C, 1 min at 55 °C and 3 min at 72 °C, followed by 13–20 cycles of 30 s at 94 °C, 30 s at 55 °C and 3 min (+5 s in each cycle) at 72 °C and finally 7 min at 72 °C. PCR cycles were adjusted when needed to decrease nonspecific products. In samples, Jl1, Ag31 and O2, where PCR products were not enough to allow for further analysis, a nested PCR was performed with primers GM3 (5′-AGAGTTTGATCMTGGC-3′) (Muyzer *et al.*, 1995) and GM4 (5′-TACCTTGTTACGACTT-3′) (Kane *et al.*, 1993). The expected amplicon size was 1550–1600 bp. PCR conditions involved an initial denaturation at 94 °C for 3 min, followed by 10–13 cycles of 94 °C for 1 min, 44 °C for 1 min, 72 °C for 3 min and a final extension at 72 °C for 5 min. The total cycles for all samples for both PCRs varied from 25 cycles in Se3 to 37 cycles in Ag31 and O2. PCR products were purified using QIAquick PCR Purification Kit (Qiagen Inc., Germany) and were cloned directly using TOPO TA Kit for sequencing (Invitrogen Inc., Germany) with chemically competent cells. The insert size was checked via PCR with M13f-M13R vector-binding primers. Positive clones were grown overnight in 1.5 mL of Luria–Bertani medium containing ampicillin (100 μg mL^{-1}), and plasmids were prepared from the pelleted cells with a QIAprep Miniprep Kit (Qiagen Inc.). Plasmids were partially sequenced with primers GM4 and ITSReub (the latter used only for the 16S–ITS libraries). After alignment with SEQUENCHER 4.6 (Gene Codes Corporation) and CLUSTALW (Larkin *et al.*, 2007), manual correction, elimination of

chimeras using PINTAIL (Ashelford *et al.*, 2005) and visual examination of the alignments, clones were grouped based on a 16S rRNA gene similarity cutoff of 99% and representatives from each group were fully sequenced using primers GM5_341f, GM1R and 907R (Muyzer *et al.*, 1995). Sequencing reactions were performed using ABI BigDye and an ABI PRISM 3100 Genetic Analyzer (Applied Biosystems Inc.). Sequences were checked for closest relatives using the BLAST application and all sequences were checked for chimeras using PINTAIL. 16S rRNA gene sequences were aligned using the ARB software (Ludwig *et al.*, 2004) and the SILVA aligner application (Pruesse *et al.*, 2007). 16S rRNA gene distance matrices were calculated with the Jukes–Cantor formula and were clustered using the neighbor-joining method. The phylogenetic tree was created in ARB software (Ludwig *et al.*, 2004). Bootstrap values were obtained from 1000 replicates using similar parameters. The length of the ITS sequences was used for the identification of ARISA peaks and for the study of the microdiversity of dominant 16S rRNA gene-derived phylotypes (data not presented here). All 16S rRNA gene sequences from this study have been deposited under GenBank numbers GQ866066–GQ866111.

FISH

Fixed tissues were washed in optimal cutting temperature (OCT) cryomicrotome medium (HISTO Service, Germany) for 5 h at 4 °C and were embedded in specific plastic wells filled with OCT overnight at − 20 °C. The frozen embedded samples were sliced horizontally to the gut walls with a cryomicrotome (Microm GmbH, Germany) into 4–5-μm-thick slices. Slices were collected on Menzel-Gläser Polysine Microscope Slides (Menzel-Gläser, Germany). Catalyzed reporter deposition-FISH was performed only in sample FN2 following a protocol described previously (Fuchs *et al.*, 2005) with the following modifications. For the deactivation of endogenous peroxidases, slides were incubated for 30 min with 0.5% sodium dodecyl sulfate in methanol, followed by two washing steps of 10 min in 1 × PBS and of 3 min in sterile double-distilled water. Hybridization buffer was prepared for the respective formamide concentrations as described previously (Fuchs *et al.*, 2005). Sections were prehybridized for 15 min at 46 °C by adding hybridization buffer only. Hybridization was followed by the addition of horseradish peroxidase-labeled probe (50 ng μL^{-1}) in a 1 : 50 dilution with the respective hybridization buffer. Samples FN3, FSe1 and FSe3 were analyzed following the basic FISH protocol (Duperron *et al.*, 2006) with the appropriate concentrations of formamide (Table S3). Basic FISH was preferentially used in most of our samples because it yielded better results in terms of clearer signals, less background and the better calculation of cell dimensions. General Cy3-labeled probes were used for the *in situ* identification of Bacteria, *Alpha-*, *Beta-* and *Gammaproteobacteria*; NON338 was used for the detection of false-positive signals (Table S3). Cy3-labeled GAM42a probe was combined with non-labeled BET42a, and vice versa, as described before (Manz *et al.*, 1992). The current specificity of these probes has recently been reviewed (Amann & Fuchs, 2008). A specific probe targeting the 16S rRNA gene sequence of the dominant in September samples phylotype (Se3-204) clustering with *Mollicutes* was designed using the ARB 'probe design' function (Ludwig *et al.*, 2004). This probe (UncMol89 5′-CGTTCGCCACTAACACCAAAATC-3′) was designed in order to be specific for this phylotype and to have two or more mismatches with the sequences found in the SILVA database (Pruesse *et al.*, 2007). The probe design considered the accessibility of 16S rRNA gene probe target sites reported elsewhere (Behrens *et al.*, 2003) and the position of the specific for the *Candidatus* Bacilloplasma probe (Kostanjsek *et al.*, 2007). Optimal stringency conditions were determined for the new probe by checking the signal intensities at increasing formamide concentrations (0–40%). The highest formamide concentration where signals were detected was 40%. However, these signals were weak, and finally 35% was chosen for the rest of the analysis. Four gut samples were analyzed, two from August 2007 (FN2, FN3) and two from September 2007 (FSe1, FSe3). Samples were visualized using an Axioplan II Imaging epifluorescence microscope (Carl Zeiss, Jena, Germany), and pictures were realized using software AXIOVISION Rel. 4.7.2 (Carl Zeiss).

Results

Analysis of shifts in community structure

The ARISA profiles generated from the bacterial communities associated with the midgut tissue of *N. norvegicus* showed high variability between samples. None of the ARISA fragments were present in all samples and the number of operational taxonomic units (OTUs) varied between 43 (sample My44) and 147 (D2) (average 91). When the complexity of the community profile was reduced by NMDS (Fig. 1), sampling time emerged as an important factor (ANOSIM $R = 0.5531$, $P < 0.001$). Morphometric factors did not significantly explain changes in microbial community structures ($P > 0.05$). Further pairwise comparisons showed that gut bacterial communities varied significantly ($P < 0.05$) between almost all months (Table 1), with either strong community differentiation ($R > 0.75$) or with differentiated, yet overlapping structure ($0.50 < R < 0.75$). The R values for the ANOSIM tests between August, September, October and December indicated largely overlapping structure ($R < 0.5$), with only the exception of the December–September comparison. No group separation was observed between the sample pairs February/March–July ($P = 0.198$) and August–October

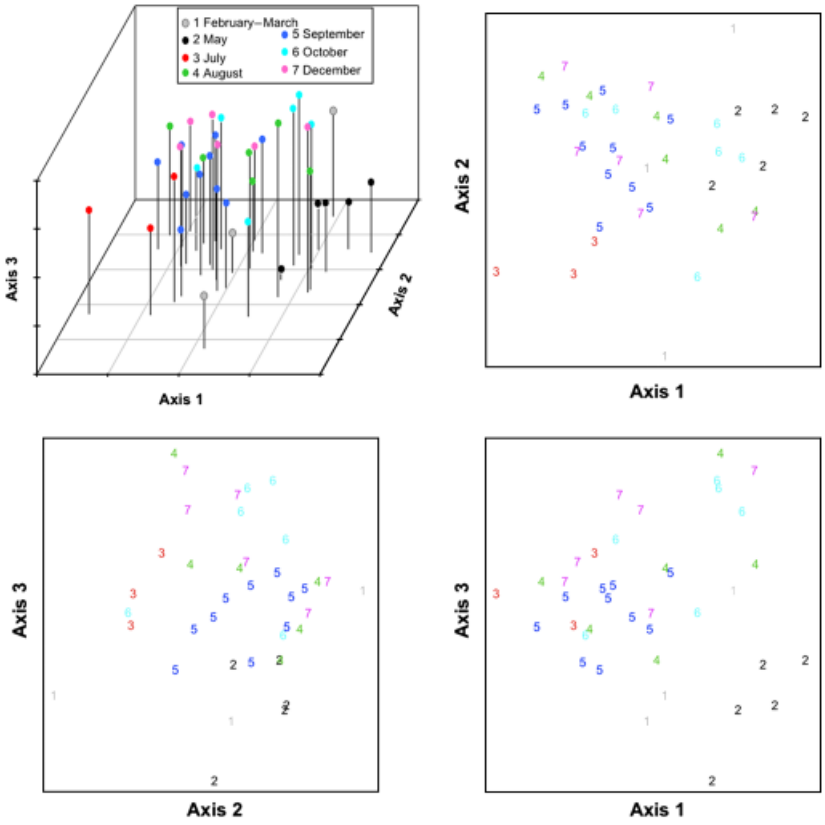

Fig. 1. NMDS ordination plots (Bray–Curtis distance matrix) of merged ARISA profiles for the *Nephrops norvegicus* gut-derived samples (ordination stress = 0.17). Each month is indicated by a different color with filled circle or number: (1) gray, February–March; (2) black, May; (3) red, July; (4) green, August; (5) blue, September; (6) light blue, October; and (7) pink, December. (a) provides three-dimensional representation of the results, (b)–(d) represent separate two-dimensional plots for all combinations of the three NMDS axes. NMDS axes are arbitrary, so that plots may arbitrarily be rotated, centered or inverted.

Table 1. ANOSIM results for the *a priori* determined temporal groups

	February/March	May	July	August	September	October	December
February/March		*0.0166*	0.1983	*0.0484*	*0.0083*	*0.0231*	*0.0105*
May	**0.5897**		*0.0183*	*0.0044*	*0.0002*	*0.0026*	*0.0023*
July	**0.4444***	**0.9692**		*0.0113*	*0.0027*	*0.013*	*0.0133*
August	**0.3765***	**0.6053**	**0.6543**		*0.0138*	0.0916	*0.0154*
September	**0.7208**	**0.9389**	**0.8403**	**0.2933***		*0.0043*	*0.0003*
October	**0.5000**	**0.8720**	**0.6975**	**0.1611***	**0.4028***		*0.0302*
December	**0.6111**	**0.9227**	**0.7654**	**0.3870***	**0.5206**	**0.2796***	

*Largely overlapping groups.

Significant noncorrected *P*-values ($P < 0.05$) are indicated with italics, significant Bonferroni corrected *P*-values ($P < 0.0024$) are underlined (upper right triangle) and *R* values are in bold (lower left triangle).

($P = 0.092$). When applying a Bonferroni correction for the 21 comparisons being made, a clear separation only occurred between all pairwise comparisons involving May, September and December samples. As mentioned above, the Bonferroni correction has often been judged to be overly conservative (Legendre & Legendre, 1998), and so care should be taken when applied to ecological data.

Phylogenetic analysis

Seven samples from different sampling seasons (Table S2) were further analyzed with the construction of clone libraries. A total of 311 full-length 16S rRNA gene sequences were determined for samples F1 (31), MY46 (58), Jl1 (30), Ag31 (22), Se3 (53), O2 (25) and D1 (92). In each clone library, 5–10 different phylotypes were detected based on a cutoff similarity of 99% (Table 2, Fig. 2). All clone libraries had a satisfactory coverage (Fig. S1) according to Good's C estimator (Kemp & Aller, 2004). Almost all clone libraries had coverage higher than 90%, apart from February (77%) and August (82%).

Except for clone library Ag31 that had two dominant phylotypes with a frequency of 31% and 27%, all clone libraries were dominated by a single phylotype being present

Table 2. 16S rRNA gene phylotypes detected in midgut samples of *Nephrops norvegicus* individuals

Phylotype	Frequency (%)	Name of closest relative	GenBank accession no.	Similarity (%)	Phylogenetic affiliation
F1-5	58.1	*Pseudoalteromonas* sp. NPO-Jl-58	AY745828	99	*Gammaproteobacteria*
F1-4	12.9	*Psychrobacter aquimaris*, KOPRI 24929	EF101547	99	*Gammaproteobacteria*
F1-7	6.4	Uncultured actinobacterium	EU374093	97	*Actinobacteria*
F1-2	3.2	Uncultured bacterium	FJ203056	96	*Gammaproteobacteria*
F1-6	3.2	Uncultured bacterium	FJ545576.1	96	*Acidobacteria*
F1-18	3.2	Uncultured *Chloroflexi*	DQ811871	98	*Chloroflexi*
F1-19	3.2	Uncultured acidobacterium	DQ395041	96	*Acidobacteria*
F1-20	3.2	Uncultured actinobacterium	EF208654	96	*Actinobacteria*
F1-26	3.2	Uncultured actinobacterium	EU374093	99	*Actinobacteria*
F1-28	3.2	Uncultured bacterium	FJ695595	98	*Gammaproteobacteria*
My46-424	74.1	*Psychrobacter* sp. Pi 2-33	AB365059	99	*Gammaproteobacteria*
My46-492	19.0	*Vibrio lentus*	AY292936	99	*Gammaproteobacteria*
My46-460	3.4	*Vibrio lentus*	AY292936	99	*Gammaproteobacteria*
My46-442	1.7	*Planococcus rifitiensis* strain M8	AJ493659	99	*Firmicutes*
My46-484	1.7	Uncultured bacterium	AB255057	98	*Firmicutes*
Jl1-36	73.3	*Photobacterium leiognathi*	AY292917	99	*Gammaproteobacteria*
Jl1-4	13.3	*Photobacterium* sp. JT-ISH-224	AB293986	99	*Gammaproteobacteria*
Jl1-1	6.6	*Photobacterium leiognathi* strain RM1	AY292947	99	*Gammaproteobacteria*
Jl1-22	3.3	*Psychrobacter aquimaris*	EF101547	99	*Gammaproteobacteria*
Jl1-28	3.3	Uncultured bacterium clone CK_1_C4_1	EU488044	87	*Firmicutes*
Ag31-3	31.9	*Photobacterium leiognathi* strain RM1	AY292947	99	*Gammaproteobacteria*
Ag31-6	27.3	*Photobacterium leiognathi*	AY292917	98	*Gammaproteobacteria*
Ag31-15	13.6	*Vibrio lentus*	AY292936	98	*Gammaproteobacteria*
Ag31-2	9.1	Uncultured bacterium	AB255065	99	*Gammaproteobacteria*
Ag31-1	4.5	*Vibrio parahaemolyticus* RIMD 2210633	BA000031	99	*Gammaproteobacteria*
Ag31-21	4.5	*Vibrio splendidus* LGP32 chromosome 1	FM954972	98	*Gammaproteobacteria*
Ag31-22	4.5	*Vibrio salmonicida* isolate PB1-8rrnB	EU091324	99	*Gammaproteobacteria*
Ag31-13	4.5	*Photobacterium* sp. HAR23	AB038031	99	*Gammaproteobacteria*
Se3-204	83.0	Uncultured *Mollicutes*	DQ340200	90	*Mollicutes*
Se3-206	5.6	*Desulfatibacillus olefinivorans* strain LM2801	DQ826724	87	*Deltaproteobacteria*
Se3-199	3.8	*Ralstonia* sp. FRA01	AF098288	99	*Betaproteobacteria*
Se3-178	3.8	*Dechloromonas* sp. HZ	AF479766	98	*Betaproteobacteria*
Se3-129	1.9	Uncultured bacterium clone CK_1_C4_19	EU488044	87	*Mollicutes*
Se3-157	1.9	Uncultured bacterium	AY328732	99	*Alphaproteobacteria*
O2-1	76.0	*Photobacterium leiognathi* strain RM1	AY292947	99	*Gammaproteobacteria*
O2-8	16.0	*Vibrio splendidus* isolate PB1-10rrnH	EU091332	99	*Gammaproteobacteria*
O2-23	4.0	*Vibrio salmonicida* isolate PB1-8rrnB	EU091324	99	*Gammaproteobacteria*
O2-37	4.0	Uncultured bacterium	EF123487	98	*Gammaproteobacteria*
D1-695	86.0	Uncultured bacterium clone CK_1_C4_1	EU488044	87	*Firmicutes*
D1-668	2.2	*Dechloromonas* sp. HZ	AF479766	99	*Betaproteobacteria*
D1-669	2.2	Arctic sea ice bacterium	AF468382	99	*Gammaproteobacteria*
D1-715	2.2	*Psychrobacter celer*	EF101550	98	*Gammaproteobacteria*
D1-727	2.2	Uncultured bacterium	EU137440	99	*Actinobacteria*
D1-684	1.1	*Psychromonas japonica*	AB304804	98	*Gammaproteobacteria*
D1-674	1.1	*Shewanella woodyi* ATCC 51908	CP000961	99	*Gammaproteobacteria*
D1-700	1.1	*Burkholderia phytofirmans* PsJN	CP001053	98	*Betaproteobacteria*

For sample code, see text. Closest relative determined via BLAST top score and phylogenetic affiliation via tree reconstruction (see Fig. 2).

with a frequency of 56–87%. All clone libraries were either dominated by sequences affiliated with *Gammaproteobacteria* (F1, My46, Jl1, Ag31, O2) or *Mollicutes* (Se3, D1). Other phylotypes detected in lower abundances were clustered with *Firmicutes*, *Actinobacteria*, *Acidobacteria*, *Chloroflexi*, *Alpha-*, *Beta-* and *Deltaproteobacteria*. Sample F1 had one dominant phylotype (F1-5, frequency 58.06%) with 99% similarity with *Pseudoalteromonas* sp. NPO-Jl-58, a heterotroph isolated from the North Pacific Ocean (Du *et al.*, 2006). The two closest known species were

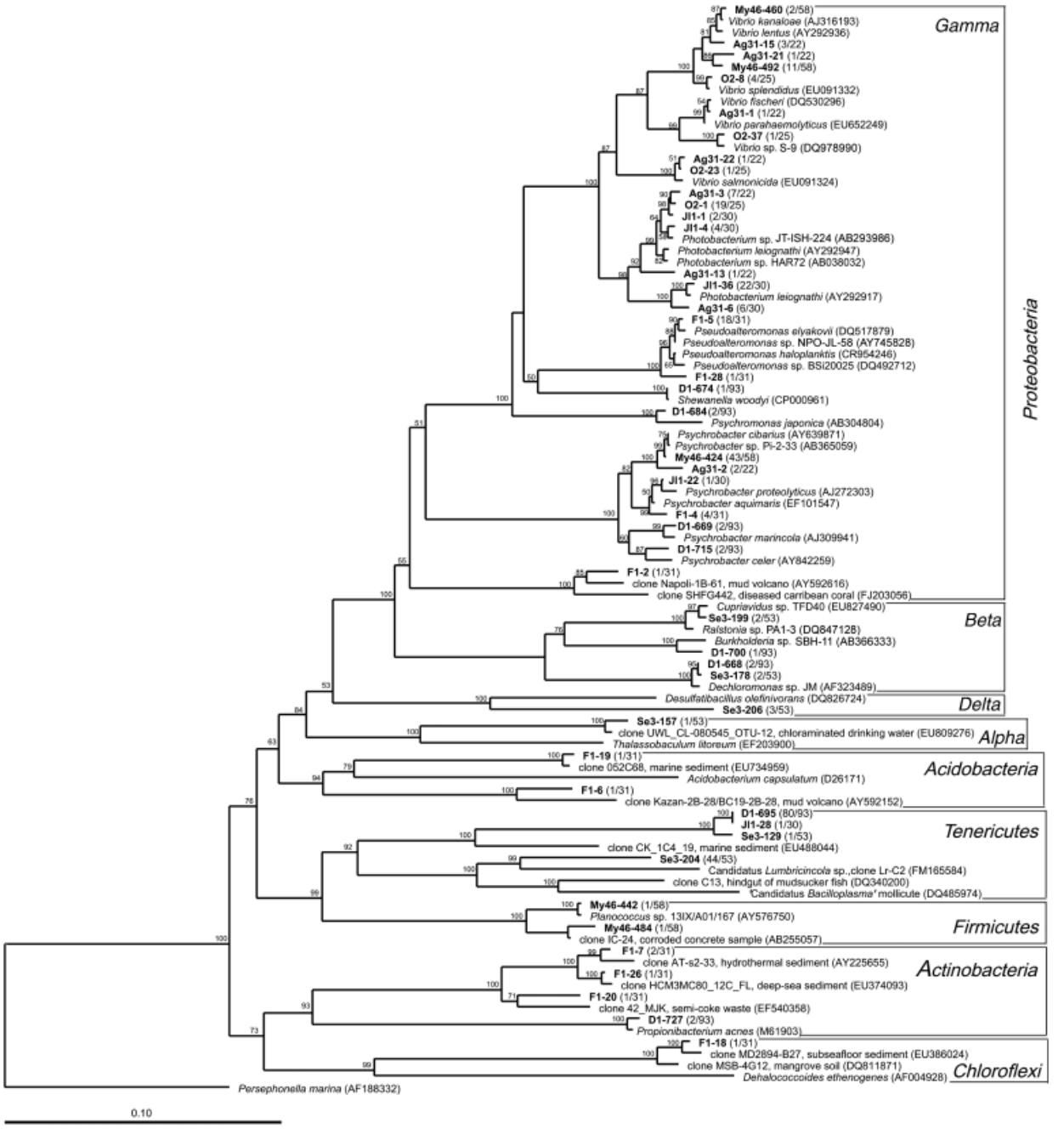

Fig. 2. Neighbor-joining tree based on 16S rRNA gene sequences from the midgut of *Nephrops norvegicus*. *Persephonella marina* (*Aquificae*) was used as an outgroup. The bar corresponds to 10% nucleotide difference and bootstrap values were calculated from 1000 replicate trees. Relative abundances of retrieved phylotypes in each clone library are shown in parentheses. Only bootstrap values over 50% are shown in the tree.

Pseudoalteromonas haloplanktis TAC125 (Medigue *et al*., 2005) and *Pseudoalteromonas elyakovii* (Sawabe *et al*., 2000), exhibiting alginolytic activity.

Sample My46 had one dominant phylotype (My46-424, frequency 72%) with 99% similarity with *Psychrobacter* sp. Pi 2-33 (Romanenko *et al*., 2008). This strain was isolated from coastal sea ice, and although not fully characterized, it was positively tested for lipolytic activity and the reduction of nitrate to nitrite. The closest fully characterized relative was *Psychrobacter cibarius* strain JG-220 isolated from fermented seafood (Jung *et al*., 2005), exhibiting lipolytic activity as well. A closely related phylotype

(Ag31-2, 98% similarity) was detected in Ag31 in a lower frequency (9%).

Samples Jl1, Ag31 and O2 were dominated by phylotypes clustering with the genus *Photobacterium* and showing $>$ 96% similarity between them (Table S4). The closest cultured relatives were a free-living strain, *Photobacterium leiognathi* RM1, isolated from the light organs of the squid *Rondeletiola minor* (Nishiguchi & Nair, 2003), *Photobacterium* sp. JT-ISH-224, isolated from the gut of the Japanese barracuda (Tsukamoto *et al.*, 2008) and *Photobacterium* sp. HAR23, isolated from the north-west Pacific Ocean water column (Urakawa *et al.*, 1999).

Sample Se3 was clearly dominated by phylotype Se3-204 (83% frequency), which clustered in a group of uncultured *Mollicutes* affiliated as a sister group of the *Mycoplasma* clade and consisting of bacteria found in the intestinal tracts of various terrestrial and marine animals (Fig. S2). Se3-204 was only 89% similar with an uncultured *Mollicutes* bacterium detected in high abundances in the gut of the long-jawed mudsucker *Gillichtys mirabilis* (Bano *et al.*, 2007). Other representatives of this group have been found in the intestine of notothenioid fishes (Ward *et al.*, 2009), the gut of *Lumbricidae* earthworms (Nechitaylo *et al.*, 2009) and the isopod *Porcellio scaber* (Kostanjsek *et al.*, 2007).

The dominant phylotype of sample D1 (D1-695, frequency 86%) fell within a highly divergent group of uncultured *Mollicutes* (Fig. S2). The representatives of the group, showing high heterogeneity between them, originate from various habitats including mammals' feces (Ley *et al.*, 2008), humans' intestinal tract where they were related to obesity (Ley *et al.*, 2006) and sediment samples (Green-Garcia, 2008). D1-695 showed low similarity (87%) with its closest relative, phylotype CK_1C4_19, found in sea-grass bed sediment from the Gulf of Mexico (Green-Garcia, 2008). Phylotypes Jl1-28 and Se3-129, found in low abundances in samples Jl1 and Se3 (3.3% and 1.5%, respectively), were 99% similar with D1-695 and with each other. Because of the low percentages of similarity with their closest relatives, both phylotypes were thoroughly checked for chimeras with the PINTAIL tool. The phylogenetic analysis (alignment) showed the presence of stem areas with large insertions. Moreover, the 'abnormalities' in the 16S rRNA gene sequences were further confirmed with the mismatches found with universal bacterial primers and probes such as EUB (I-III), ITSF and GM5_341f (Table S5).

FISH

No signals were detected with the negative control NON338 and with probe BET42a. Hybridization experiments with probes EUB338 (I-III) and GAM42a were positive in samples FN2 and FN3. The cells detected were mostly curved rods (4 μm $\times$ 1.5 μm) and were located in the internal gut wall (Fig. 3a). Hybridization experiments with the newly designed UncMol89 probe, targeting phylotype Se3-204, were positive in FSe1 and FSe3. The cells detected were packages of cocci organized in groups of four cells or eight cells (each cell around 1.5 μm) (Figs 3b and S3), a sarcina morphotype, which is not consistent with that of known *Mollicutes*. They were located in the internal wall surface of the gut and showed a patchy distribution. Such distribution has been described previously for another uncultured gut *Mollicutes* (Kostanjsek *et al.*, 2007). Very few signals were detected with probe EUB338 (I-III) in samples FSe1 and FSe3 and showed a different morphotype to the sarcina detected with probe UncMol89. The sarcina morphotype was detected on the same sections only through DAPI signals, suggesting the weak binding of EUB338 (I-III) to the unknown bacteria.

Discussion

This study analyzed the temporal variability throughout a year of gut microbial communities of *N. norvegicus* individuals along with their morphometric characteristics in order

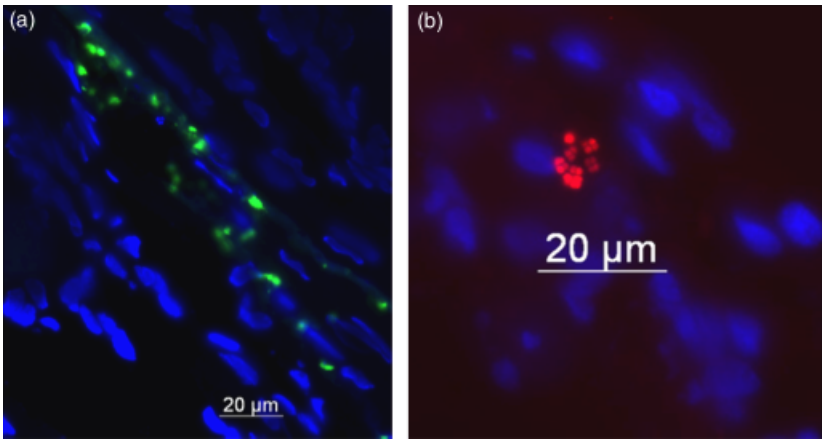

Fig. 3. (a) Gut section (thickness 5 μm) of *Nephrops norvegicus* sample FN2 (August) hybridized with horseradish peroxidase-labeled GAM42a probe specific for *Gammaproteobacteria*, and stained with Alexa488-labeled tyramide. Blue signal corresponds to DAPI signal from the gut-wall epithelial cells and green signal corresponds to the hybridized bacteria. (b) Gut section (thickness 4 μm) of *N. norvegicus* sample FSE3 (September) hybridized with Cy3-labeled probe UncMol89 specific for uncultured *Mollicutes* phylotype Se3-204 detected in this study. Blue signal corresponds to DAPI signal from the gut-wall epithelial cells and red signal corresponds to the hybridized bacteria.

to reveal the factors that might influence their gut microbial diversity. None of the morphological factors could explain significantly the bacterial community shifts, while a temporal pattern of variation was observed (Fig. 1; Table 1). The *a priori* hypothesis that gut microbial communities may show a temporal pattern was based on the temporal changes in food availability, which has been shown to potentially influence the gut microbiota (Harris, 1993; Lau *et al.*, 2002; Ley *et al.*, 2008 and references therein). Hence, ecosystem seasonal fluctuations (e.g. phytoplankton bloom) result in differential food availability and quality, whose exact components are still to be determined. Combining the feeding behavior of *N. norvegicus* acting either as a predator (small mollusks, crustaceans and polychaetes) or as a scavenger (fish, bigger invertebrates), with the periodicity observed in the system of Pagasitikos Gulf, it is assumed that the highest quality of available food for *N. norvegicus* would occur around April–May and would slowly decrease till the next bloom.

Interestingly, the above-mentioned fluctuations in food quality and quantity were reflected at the level of microbial community structure (Table 1), not at the onset of the food changes, but a few months later. Indeed, bacterial communities presented a different structure but some degree of overlap ($R = 0.5897$; $P = 0.0166$) between February/March (maximum phytodetritus season) and May (highest food quality and availability). However, it was only after May that the structures of the gut bacterial communities were drastically affected ($R = 0.969$ between May and July). July–August could further represent a transition zone where food still decreases in abundance or quality and thus slight changes in community structures are still observed ($R = 0.6543$). From August to December, when food becomes scarce, there is no drastic change in diet and the gut bacterial communities would not differentiate considerably ($R < 0.41$). These hypotheses were also supported by analyzing the microbial OTU turnover between any two consecutive months (Fig. 4). Between February and August, bacterial communities became gradually more and more dissimilar (> 40–55% replacement of the OTUs each time), while after August, no further variation was evidenced ($< 30\%$ turnover).

Noticeably, the results of the clone libraries and FISH experiments, for representatives of these groups, showed that December and September samples were dominated by uncultured *Mollicutes* while August and October samples contained more *Gammaproteobacteria*. The *in silico* analysis for both *Mollicutes* dominant phylotypes showed that the ITSF primer used in this study for ARISA had three mismatches with the binding site (Table S5). The ITS length found for the two dominant phylotypes, Se3-204 and D1-695, was 317 and 246 bp, respectively. These two ITS sizes were found in the ARISA tables showing very low relative area values ($< 0.5\%$) (data not shown in this study).

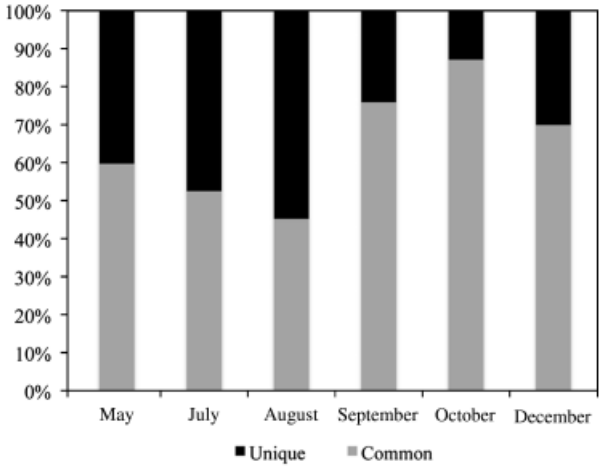

Fig. 4. Relative abundance of common bacterial OTUs from the midgut of *Nephrops norvegicus* between two consecutive months' samples as calculated from the ARISA experiments. The percentage of phylotypes that is shared with the previous month's samples is designated with light gray. February/March is not shown because there was no previous month with which it could be compared.

Consequently, the *Mollicutes*' microdiversity is not totally represented in the NMDS plot due to PCR and primer biases. In order to design a novel forward ARISA primer targeting at the same time *Mollicutes* and the rest of the Bacteria, a primer with three degenerate positions at the 3′ primer end with one of them being degenerate for more than two nucleotides (Table S5) would be needed. Because this could lead to additional PCR biases, the testing of such a primer will be addressed in our future research. Apart from this technical consideration, further comparisons between the two techniques (ARISA and clone libraries) are not presented, because the two approaches describe fundamentally different components of the diversity of microbial communities (Bent & Forney, 2008). In addition, ARISA was performed on the ITS level, while sequencing was performed on the 16S and ITS levels; therefore, not only the techniques differed but also the targeted molecular markers. It is then not surprising that a discrepancy between the clone libraries and the ARISA results may be evidenced for OTU numbers. Indeed, it is conceivable that a given 16S rRNA gene sequence might occur in many samples, but could be associated with different ITS sequences (representing intra- or intergenomic variability), the latter being associated only with specific samples.

The clone libraries analysis showed one or two dominant phylotypes for each sample (Table 2), suggesting rather specialized bacterial communities. February was dominated by a *Pseudoalteromonas*-like phylotype. Members of this genus are associated with higher organisms, have the ability of easily colonizing surfaces and display antibacterial, bacteriolytic, agarolytic and algicidal activities (Holmstrom &

Kjelleberg, 1999). Although *N. norvegicus* does not feed on algae, remains of plants can be found in its stomach (Cristo & Cartes, 1998) probably due to passive ingestion. The presence of *Pseudoalteromonas*-like organisms could be related to the presence of algal material in the intestine of *N. norvegicus* assisting in its decomposition. In addition, the second most dominant phylotype in the same sample was closely related to a *Psychrobacter aquimaris* strain, originating from a marine alga, enhancing the inferred alginolytic character of the bacterial community.

Another *Psychrobacter*-like phylotype, with potential lipolytic activity, dominated in May. Members of this genus have been found in a wide range of environments, such as sea ice, sea water, marine sediments, salt marshes, ornithogenic soils, food microbiota, animal tissues and sponges (Bowman, 2006). For example, *Psychrobacter proteolyticus* has been isolated from the gut of the krill *Euphausia superba* (Denner *et al.*, 2001). The lipolytic activity inferred from its closest relatives, combined with the expected high food availability, indicates that lipid digestion is feasible.

The July, August and October communities were dominated by highly similar phylotypes of the genus *Photobacterium* (Tables 2 and S4). Representatives of this genus show fermentative metabolism and are isolated from the light organs of several marine animals. However, bioluminescent bacteria are ubiquitous in fish intestinal tracts, being the most abundant aerobes in such habitats (Farmer & Hickman-Brenner, 2006; Ward *et al.*, 2009). Biochemical studies proved chitinase activity and lipase activity in 96% and 82% of *P. leiognathi* strains, respectively (Farmer & Hickman-Brenner, 2006). Strains of *Photobacterium phosphoreum* have characteristics similar to that of *P. leiognathi* including chitinase activity. Although we did not investigate lipase or chitinase activity in our samples, the dominance ($>60\%$) of almost identical phylotypes in three different months reveals a specialized community. The phylotypes detected were closely related, as described above, to *Photobacterium* sp. isolated from tissues of marine animals enhancing the hypothesis of their ability to colonize the *N. norvegicus* gut.

After the summer, phylotypes Se3-204 and D1-695 clustered within two groups of uncultured *Mollicutes* (Fig. S2). Many members of *Mollicutes* are obligate intracellular symbionts that possess the smallest genomes of self-replicating organisms (Razin *et al.*, 1998). Some mycoplasmas are known pathogens, but many species appear to be simply part of the natural microbiota of their hosts and seem to have no harmful effects on the host (Giebel *et al.*, 1990). No physiological properties can be inferred for the found *Mollicutes*-related phylotypes, because they share $<83\%$ similarity with cultured representatives. Moreover, it has been suggested that members from the two groups of uncultured *Mollicutes* to which the phylotypes of this study belonged (Fig. S2) may represent only a small part of an as-yet-uncultured bacterial lineage colonizing the intestines of various arthropods and vertebrate hosts (Kostanjsek *et al.*, 2007). Importantly, these bacteria do not seem to have a parasitic relationship with their hosts, because in most cases, the animals that harbored were healthy (Bano *et al.*, 2007; Kostanjsek *et al.*, 2007; Nechitaylo *et al.*, 2009; Ward *et al.*, 2009).

The FISH specificity of UncMol89, targeting Se3-204 was only tested *in silico* and not empirically. However, the consistent sarcina morphotype detected with UncMol89 and the expected absence of EUB338 (I-III) signals of this specific morphotype (Table S5) argues in favor of sequence Se3-204 originating from the sarcina morphotypes. Although probe UncMol89 had minimum two mismatches with the 'closely' related gut uncultured *Mollicutes* and more than three mismatches to all other known sequences, additional experiments such as the design of nonlabeled competitor probes for the blocking of non-target-binding sites (Manz *et al.*, 1992) should be used in future experiments to ensure the origin of the Se3-204 phylotype from the sarcina cells.

Other ways to better test the specificity of UncMol89 would be the design of a modified UncMol89 with two to three mismatches to the Se3-204 phylotype where diminished probe signaling from the sarcina cells would be expected. Alternatively, UncMol89 could be tested against cultured organisms with two or more mismatches to test whether probe signaling disappears. The absence of signals from the sarcina cells when using EUB338 (I-III) could be explained by the two central mismatches of the probe with the 16S rRNA gene sequence of the phylotype Se3-204 (Table S5). The design of modified EUB probes correcting the mismatches with Se3-204 and resulting in better probe signalling for the sarcina cells would further confirm their origin from Se3-204.

Phylotypes clustering within the genus *Vibrio* were present in most of the samples, showing low (3.5%) to moderate (19.0%) relative abundance. The majority of their closest relatives originated from marine animals (Nasu *et al.*, 2000; Nishiguchi & Nair, 2003; Jensen *et al.*, 2009). This genus is often found in associations with the gut of marine animals varying from parasitism to mutualism and showing diverse metabolic capabilities (Thompson *et al.*, 2004).

The rest of the phylotypes clustered within the groups of *Actinobacteria*, *Acidobacteria*, *Chloroflexi*, *Firmicutes*, *Alpha-*, *Beta-* and *Deltaproteobacteria*. These phyla dominate frequently in sediment samples. Their low presence could be attributed to remains of sediment particles of ingested food that were not removed by the mechanical evacuation and the rinsing of the gut.

Overall, most of the phylotypes found were associated either with the intestinal tract of marine animals or with their light organs. Consequently, it is most likely that these

phylotypes have the ability to attach to tissue surfaces and successfully colonize the midgut. Some of the phylotypes could also be pathogens, although all animals collected were healthy. The presence of highly similar ($\geq$99%) phylotypes in different months at varying frequencies (Tables 2 and S4, Fig. 2) indicates that at least the dominant phylotypes may be present throughout the year, despite fluctuating environmental conditions. The existence of these recurring phylotypes indicates that these bacteria might be representative of specific communities or even participate in symbiotic interactions, i.e. resident bacteria, with *N. norvegicus*. More specifically, the *Gammaproteobacteria* detected are universally dispersed in different animals and varying habitats and appear in *N. norvegicus*' gut at different abundances throughout the year. The hypothesis of the temporal effect of the trophic state of the overlying water column on the gut microbial communities, which this study supports, needs to be further investigated with feeding experiments and estimation of prey availability or phytodetritus flux.

Acknowledgements

We acknowledge support from the International Max Planck Research School of Marine Microbiology (MarMic), the Deutscher Academischer Austausch Dienst (DAAD). Part of this research was cofunded by the European Social Fund & National Resources EPEAK II-PYTHAGORAS II. Rudolf Amann is acknowledged for advice on FISH and for his comments on the manuscript. We also thank two anonymous reviewers for their comments.

References

Amann R & Fuchs BM (2008) Single-cell identification in microbial communities by improved fluorescence *in situ* hybridization techniques. *Nat Rev Microbiol* **6**: 339–348.

Ashelford KE, Chuzhanova NA, Fry JC, Jones AJ & Weightman AJ (2005) At least 1 in 20 16S rRNA sequence records currently held in public repositories is estimated to contain substantial anomalies. *Appl Environ Microb* **71**: 7724–7736.

Bano N, DeRae Smith A, Bennett W, Vasquez L & Hollibaugh JT (2007) Dominance of Mycoplasma in the guts of the Long-Jawed Mudsucker, *Gillichthys mirabilis*, from five California salt marshes. *Environ Microbiol* **9**: 2636–2641.

Behrens S, Ruhland C, Inacio J, Huber H, Fonseca A, Spencer-Martins I, Fuchs BM & Amann R (2003) *In situ* accessibility of small-subunit rRNA of members of the domains Bacteria, Archaea, and Eucarya to Cy3-labeled oligonucleotide probes. *Appl Environ Microb* **69**: 1748–1758.

Bell MC, Redant F & Tuck I (2006) *Nephrops* species. *Lobsters: biology, management, aquaculture and fisheries* (Phillips BF, ed), pp. 412–469. Blackwell, Oxford.

Bent SJ & Forney LJ (2008) The tragedy of the uncommon: understanding limitations in the analysis of microbial diversity. *ISME J* **2**: 689–695.

Boer SI, Hedtkamp SIC, van Beusekom JEE, Fuhrman JA, Boetius A & Ramette A (2009) Time- and sediment depth-related variations in bacterial diversity and community structure in subtidal sands. *ISME J* **3**: 780–791.

Bowman JP (2006) The genus *Psychrobacter*. *The Prokaryotes* (Dworkin M, Falkow S, Rosenberg E, Schleifer K-H & Stackenbrandt E, eds), pp. 920–930. Springer, New York.

Cardinale M, Brusetti L, Quatrini P, Borin S, Puglia AM, Rizzi A, Zanardini E, Sorlini C, Corselli C & Daffonchio D (2004) Comparison of different primer sets for use in automated ribosomal intergenic spacer analysis of complex bacterial communities. *Appl Environ Microb* **70**: 6147–6156.

Clarke KR (1993) Non-parametric multivariate analyses of changes in community structure. *Aust J Ecol* **18**: 117–143.

Clarke KR & Green RH (1988) Statistical design and analysis for a biological effects study. *Mar Ecol-Prog Ser* **46**: 213–226.

Cristo M & Cartes JE (1998) A comparative study of the feeding ecology of *Nephrops norvegicus* (L.), (Decapoda: Nephropidae) in the bathyal Mediterranean and the adjacent Atlantic. *Sci Mar* **62**: 81–90.

Denner EB, Mark B, Busse HJ, Turkiewicz M & Lubitz W (2001) *Psychrobacter proteolyticus* sp. nov., a psychrotrophic, halotolerant bacterium isolated from the Antarctic krill *Euphausia superba* Dana, excreting a cold-adapted metalloprotease. *Syst Appl Microbiol* **24**: 44–53.

Du HL, Jiao NZ, Hu YH & Zeng YH (2006) Diversity and distribution of pigmented heterotrophic bacteria in marine environments. *FEMS Microbiol Ecol* **57**: 92–105.

Duperron S, Bergin C, Zielinski F, Blazejak A, Pernthaler A, McKiness ZP, DeChaine E, Cavanaugh CM & Dubilier N (2006) A dual symbiosis shared by two mussel species, *Bathymodiolus azoricus* and *Bathymodiolus puteoserpentis* (Bivalvia: Mytilidae), from hydrothermal vents along the northern Mid-Atlantic Ridge. *Environ Microbiol* **8**: 1441–1447.

Farmer JJ III & Hickman-Brenner FW (2006) The genera *Vibrio* and *Photobacterium*. *The Prokaryotes* (Dworkin M, Falkow S, Rosenberg E, Schleifer K-H & Stackenbrandt E, eds), pp. 508–563. Springer, New York.

Fisher MM & Triplett EW (1999) Automated approach for ribosomal intergenic spacer analysis of microbial diversity and its application to freshwater bacterial communities. *Appl Environ Microb* **65**: 4630–4636.

Fuchs BM, Woebken D, Zubkov MV, Burkill P & Amann R (2005) Molecular identification of picoplankton populations in contrasting waters of the Arabian Sea. *Aquat Microb Ecol* **39**: 145–157.

Giebel J, Binder A & Kirchhoff H (1990) Isolation of *Mycoplasma moatsii* from the intestine of wild Norway rats (*Rattus norvegicus*). *Vet Microbiol* **22**: 23–29.

Green-Garcia AM (2008) Characterization of the Lucinid bivalve-bacteria symbiotic system: the significance of the geochemical

habitat on bacterial symbiont diversity and phylogeny. MSc Thesis, Louisiana State University, Baton Rouge, LA.

Harris JM (1993) The presence, nature, and role of gut microflora in aquatic invertebrates: a synthesis. *Microb Ecol* **25**: 195–231.

Holmstrom C & Kjelleberg S (1999) Marine *Pseudoalteromonas* species are associated with higher organisms and produce biologically active extracellular agents. *FEMS Microbiol Ecol* **30**: 285–293.

Jensen S, Frost P & Torsvik VL (2009) The nonrandom microheterogeneity of 16S rRNA genes in *Vibrio splendidus* may reflect adaptation to versatile lifestyles. *FEMS Microbiol Lett* **294**: 207–215.

Jung SY, Lee MH, Oh TK, Park YH & Yoon JH (2005) *Psychrobacter cibarius* sp. nov., isolated from jeotgal, a traditional Korean fermented seafood. *Int J Syst Evol Micr* **55**: 577–582.

Kane MD, Poulsen LK & Stahl DA (1993) Monitoring the enrichment and isolation of sulfate-reducing bacteria by using oligonucleotide hybridization probes designed from environmentally derived 16Ss ribosomal-RNA sequences. *Appl Environ Microb* **59**: 682–686.

Kemp PF & Aller JY (2004) Estimating prokaryotic diversity: when are 16S rDNA libraries large enough? *Limnol Oceanogr-Meth* **2**: 114–125.

Kostanjsek R, Strus J & Avgustin G (2007) '*Candidatus* Bacilloplasma,' a novel lineage of *Mollicutes* associated with the hindgut wall of the terrestrial isopod *Porcellio scaber* (Crustacea: Isopoda). *Appl Environ Microb* **73**: 5566–5573.

Kruskal JB (1964) Multidimensional scaling by optimizing a goodness of fit to a nonmetric hypothesis. *Psychometrika* **29**: 1–28.

Lane DJ (1991) 16S/23S rRNA sequencing. *Nucleic acid techniques in bacterial systematics* (Stackenbrandt E & Goodfellow M, eds), pp. 115–175. John Wiley & Sons, Chichester.

Larkin MA, Blackshields G, Brown NP *et al.* (2007) Clustal W and clustal X version 2.0. *Bioinformatics* **23**: 2947–2948.

Lau WWY, Jumars PA & Armbrust EV (2002) Genetic diversity of attached bacteria in the hindgut of the deposit-feeding shrimp *Neotrypaea* (formerly *Callianassa*) *californiensis* (Decapoda: Thalassinidae). *Microb Ecol* **43**: 455–466.

Legendre P & Legendre L (1998) *Numerical Ecology*, 2nd edn. Elsevier, Amsterdam.

Ley RE, Turnbaugh PJ, Klein S & Gordon JI (2006) Microbial ecology: human gut microbes associated with obesity. *Nature* **444**: 1022–1023.

Ley RE, Hamady M, Lozupone C *et al.* (2008) Evolution of mammals and their gut microbes. *Science* **320**: 1647–1651.

Loo LO, Baden SP & Ulmestrand M (1993) Suspension-feeding in adult *Nephrops norvegicus* (L.) and *Homarus gammarus* (L.) (decapoda). *Neth J Sea Res* **31**: 291–297.

Ludwig W, Strunk O, Westram R *et al.* (2004) ARB: a software environment for sequence data. *Nucleic Acids Res* **32**: 1363–1371.

Manz W, Amann R, Ludwig W, Wagner M & Schleifer K-H (1992) Phylogenetic oligodeoxynucleotide probes for the major subclasses of Proteobacteria: problems and solutions. *Syst Appl Microbiol* **15**: 593–600.

Medigue C, Krin E, Pascal G *et al.* (2005) Coping with cold: the genome of the versatile marine Antarctica bacterium *Pseudoalteromonas haloplanktis* TAC125. *Genome Res* **15**: 1325–1335.

Muyzer G, Teske A, Wirsen CO & Jannasch HW (1995) Phylogenetic-relationships of *Thiomicrospira* species and their identification in deep-sea hydrothermal vent samples by denaturing gradient gel-electrophoresis of 16S rDNA fragments. *Arch Microbiol* **164**: 165–172.

Nasu H, Iida T, Sugahara T, Yamaichi Y, Park KS, Yokoyama K, Makino K, Shinagawa H & Honda T (2000) A filamentous phage associated with recent pandemic *Vibrio parahaemolyticus* O3:K6 strains. *J Clin Microbiol* **38**: 2156–2161.

Nechitaylo TY, Timmis KN & Golyshin PN (2009) '*Candidatus* Lumbricincola', a novel lineage of uncultured *Mollicutes* from earthworms of family *Lumbricidae*. *Environ Microbiol* **11**: 1016–1026.

Nishiguchi MK & Nair VS (2003) Evolution of symbiosis in the Vibroonaceae: a combined approach using molecules and physiology. *Int J Syst Evol Micr* **53**: 2019–2026.

Petihakis G, Triantafyllou G, Pollani A, Koliou A & Theodorou A (2005) Field data analysis and application of a complex water column biogeochemical model in different areas of a semi-enclosed basin: towards the development of an ecosystem management tool. *Mar Environ Res* **59**: 493–518.

Pruesse E, Quast C, Knittel K, Fuchs BM, Ludwig W, Peplies J & Glockner FO (2007) SILVA: a comprehensive online resource for quality checked and aligned ribosomal RNA sequence data compatible with ARB. *Nucleic Acids Res* **35**: 7188–7196.

Ramette A (2007) Multivariate analyses in microbial ecology. *FEMS Microbiol Ecol* **62**: 142–160.

Ramette A (2009) Quantitative community fingerprinting methods for estimating the abundance of operational taxonomic units in natural microbial communities. *Appl Environ Microb* **75**: 2495–2505.

Razin S, Yogev D & Naot Y (1998) Molecular biology and pathogenicity of mycoplasmas. *Microbiol Mol Biol R* **62**: 1094–1156.

Romanenko LA, Tanaka N, Uchino M, Kalinovskaya NI & Mikhailov VV (2008) Diversity and antagonistic activity of sea ice bacteria isolated from the sea of Japan. *Microbes Environ* **23**: 209–214.

Sarda F & Valladares FJ (1990) Gastric evacuation of different foods by *Nephrops norvegicus* (Crustacea: Decapoda) and estimation of soft-tissue ingested, maximum food-intake and cannibalism in captivity. *Mar Biol* **104**: 25–30.

Sawabe T, Tanaka R, Iqbal MM, Tajima K, Ezura Y, Ivanova EP & Christen R (2000) Assignment of *Alteromonas elyakovii* KMM 162(T) and five strains isolated from spot-wounded fronds of

Laminaria japonica to *Pseudoalteromonas elyakovii* comb. nov. and the extended description of the species. *Int J Syst Evol Micr* **50**: 265–271.

Thompson FL, Iida T & Swings J (2004) Biodiversity of vibrios. *Microbiol Mol Biol R* **68**: 403–431.

Tsukamoto H, Takakura Y, Mine T & Yamamoto T (2008) *Photobacterium* sp. JT-ISH-224 produces two sialyltransferases, alpha-/beta-galactoside alpha2,3-sialyltransferase and beta-galactoside alpha2,6-sialyltransferase. *J Biochem* **143**: 187–197.

Urakawa H, Kita-Tsukamoto K & Ohwada K (1999) Restriction fragment length polymorphism analysis of psychrophilic and psychrotrophic *Vibrio* and *Photobacterium* from the northwestern Pacific Ocean and Otsuchi Bay, Japan. *Can J Microbiol* **45**: 67–76.

Ward NL, Steven B, Penn K, Methe BA & Detrich WH (2009) Characterization of the intestinal microbiota of two Antarctic notothenioid fish species. *Extremophiles* **13**: 679–685.

Yonge CM (1924) Studies on the comparative physiology of digestion: II. The mechanism of feeding, digestion, and assimilation in *Nephrops norvegicus*. *J Exp Biol* **1**: 343–389.

Supporting Information

Additional Supporting Information may be found in the online version of this article:

Figure S1. Clone library coverage based on Good's C estimator.

Figure S2. Neighbour-joining tree based on the *Mollicutes* 16S rRNA gene sequences from the midgut of *Nephrops norvegicus*.

Figure S3. Gut section (thickness 4 μm) of *Nephrops norvegicus* sample FSE3 (September) hybridized with Cy3-labeled probe UncMol89 specific for uncultured *Mollicutes* phylotype Se3-204 detected in this study.

Table S1. Morphometric data for the samples used for ARISA and clone libraries analysis.

Table S2. Samples used for DNA extraction and FISH (all DNA samples were used for ARISA analysis).

Table S3. Oligonucleotide probes used in the study.

Table S4. Pairwise comparisons of the 16S rRNA gene sequence similarities (%) of *Photobacterium* sp.-like sequences and their closest relatives: (1) *Photobacterium leiognathi* strain RM1 (AY292947), (2) *P. leiognathi* (AY292917), (3) *Photobacterium* sp. HAR23 (AB038031), (4) *Photobacterium* sp. Jt-ISH-224 (AB293986).

Table S5. *In silico* detected mismatches (underlined) of phylotypes Se3-204 and D1-695 with primers and probe EUB338 (I-III) used in this study with.

Please note: Wiley-Blackwell is not responsible for the content or functionality of any supporting materials supplied by the authors. Any queries (other than missing material) should be directed to the corresponding author for the article.

Table S1. Morphometric data for the samples used for ARISA and clone libraries analysis. Pooled samples are designated with italics, and samples analyzed with clone libraries are in boldface.

Sample	Month	Sex	Body weight (g)	Carapace length (mm)	Carapace width (mm)	Abdominal width (mm)
F40	February	M	89.91	50.21	27.47	24.57
F44	February	M	44.71	26.77	24.5	23.48
F1 (F40/F44)	***February***	***M***	***67.31***	***38.49***	***25.985***	***24.025***
Mr4	March	F	17.98	36.04	18.25	17.59
Mr10	March	F	26.31	36.4	18.6	19.8
Mr1(Mr4/Mr10)	*March*	*F*	*22.145*	*36.22*	*18.425*	*18.695*
Mr26	March	M	30.35	40.6	22.47	21.18
My27	May	F	12.47	27.32	13.95	15.33
My44	May	M	49.79	42.75	21.84	21.83
My45	May	M	27.69	36.15	18.89	18.65
My46	**May**	**M**	**29.2**	**37.22**	**17.64**	**19.22**
My47	May	M	39.21	40.36	21.3	20.63
Jl1	**July**	**F**	**38.51**	**38.54**	**20.51**	**22.57**
Jl3	July	F	65.28	48.13	25.22	26.82
Jl14	July	M	59.9	44.79	23.18	23.12
Jl17	July	M	50.38	41.92	20.78	21.41
Jl19	July	M	39.73	40.16	19.65	20.37
Jl4(Jl14/Jl17/Jl19)	*July*	*M*	*50*	*42.29*	*21.2*	*21.63*
Ag4	August	F	22.53	35.18	17.94	19.8
Ag6	August	F	28.35	35.94	18.67	19
Ag9	August	F	43.54	42.53	21.39	23.33
Ag1(Ag4/Ag6/Ag9)	*August*	*F*	*31.47*	*37.88*	*19.33*	*20.71*
Ag2.1	August	F	30.66	36.4	18.3	20.5
Ag8	August	F	23.72	32.93	16.53	18.4
Ag16	August	F	22.05	35.66	18	20.46
Ag23	August	F	31.48	37.41	18.63	21.4
Ag31	**August**	**M**	**52.58**	**42.46**	**21.34**	**21.88**
Se1	September	M	43.3	40.32	22.74	21.83
Se2	September	M	68.9	44.96	27.17	27.09
Se3	**September**	**M**	**22.297**	**31.47**	**17.59**	**17**
Se4	September	F	45.85	40.92	20.53	20.45
Se5	September	F	27.5	35.04	17.83	18.32
Se6	September	F	21.61	31.67	19.32	18.67
Se7	September	F	36.04	38.9	19.98	22.5
Se9	September	F	31.51	37.58	19.35	21.22
Se11	September	M	28.88	35.33	17.83	18.51
Se12	September	M	32.41	37.94	18.45	17.51
O1	October	F	36.71	38.36	19.21	22.11
O2	**October**	**F**	**24.8**	**35.61**	**16.44**	**19.75**
O3	October	F	17.37	29.97	14.91	16.85
O4	October	F	11.85	28.59	13.34	13.9
O5	October	M	29.12	36.84	17.72	18.53
O6	October	M	27.76	35.71	17.35	18.12
D1	**December**	**F**	**22.06**	**35.25**	**17.3**	**19.86**
D2	December	F	21.99	32.12	16.23	18.18
D3	December	F	20.77	32.18	15.51	17.17
D4	December	M	32.78	40.05	19.48	20.27
D6	December	M	59.47	45.88	24.09	23.1
D7	December	M	18.85	35	17.32	17.87

Table S2. Samples used for DNA extraction and FISH (all DNA samples were used for ARISA analysis). Samples used for the construction of the clone libraries are indicated by bold letters. F: February, Mr: March, My: May, Jl: July, Ag: August, Se: September, O: October, D: December, FN: fixed August samples, FSe: fixed September samples

Month	Sample code	Pooled samples	Fixed samples
February	-	**F1 (F40/F44)**	
March	Mr26	Mr1 (Mr4/Mr10)	
May	My27/My44/My45/**My46**/My47		
July	**Jl1**/Jl3	Jl4 (Jl14/Jl17/Jl19)	
August	Ag2.1/Ag8/Ag16/Ag23/**Ag31**	Ag1 (Ag4/Ag6/Ag9)	FN2/FN3
September	Se1/Se2/**Se3**/Se4/Se5/Se6/Se7/Se9/Se11/Se12		FSe3/FSe1
October	O1/**O2**/O3/O4/O5/O6		
December	**D1**/D2/D3/D4/D6/D7		

Table S3. Oligonucleotide probes used in the study. FA: formamide concentration.

Probe	Group specificity	Sequence (5' → 3')	*Escherichia coli* 16S or 23S rRNA position	FA%	Reference
EUB338 (I-III)	Almost all Bacteria	GCWGCCWCCCGTAGGWGT	338-355	35	Daims, *et al.*, 1999
NON338	Negative control	ACTCCTACGGGAGGCAGC	-	35	Amann, *et al.*, 1990
GAM42a	γ-Proteobacteria	GCCTTCCCACATCGTTT	helix 42a, 23S rRNA	35	Manz *et al*., 1992
BET42a	β-Proteobacteria	GCCTTCCCACTTCGTTT	helix 42a, 23S rRNA	35	Manz *et al*., 1992
ALF968 (*)	α-Proteobacteria	GGTAAGGTTCTGCGCGTT	968	35	Gloeckner, *et al.*, 1999
UncMol89	Uncult. Mollicutes	CGTTCGCCACTAACACCAAAATC	89	35	This study

*: ALF968 has low specificity as determined from database search. However in this study no signals were detected with this probe so no further checking was performed

Amann RI, Krumholz L & Stahl DA (1990) Fluorescent-oligonucleotide probing of whole cells for determinative, phylogenetic, and environmental studies in microbiology. *J Bacteriol* **172**: 762-770.

Daims H, Bruhl A, Amann R, Schleifer KH & Wagner M (1999) The domain-specific probe EUB338 is insufficient for the detection of all Bacteria: Development and evaluation of a more comprehensive probe set. *Syst Appl Microbiol* **22**: 434-444.

Glockner FO, Fuchs BM & Amann R (1999) Bacterioplankton compositions of lakes and oceans: a first comparison based on fluorescence in situ hybridization. *Appl Environ Microbiol* **65**: 3721-3726.

Manz W, Amann R, Ludwig W, Wagner M & Schleifer K-H (1992) Phylogenetic oligodeoxynucleotide probes for the major subclasses of Proteobacteria: problems and solutions. . *Syst Appl Microbiol* **15**: 593-600.

Table S4. Pairwise comparisons of the 16S rRNA gene sequence similarities (%) of *Photobacterium* sp.-like sequences and their closest relatives, 1: *Photobacterium leiognathi* strain RM1 (AY292947), 2: *P. leiognathi* (AY292917), 3: *Photobacterium* sp. HAR23 (AB038031), 4: *Photobacterium* sp. Jt-ISH-224 (AB293986). Highest similarity, 99%, is indicated in boldface. For sample codes see text.

1	2	3	4	Jl1-36	Jl1-4	Jl1-1	Ag31-3	Ag31-6	Ag31-13	O2-1	phylotypes
-	96	**99**	98	96	**99**	**99**	**99**	96	97	**99**	1
	-	96	96	**99**	96	96	96	98	96	96	2
		-	98	96	**99**	**99**	98	97	98	**99**	3
			-	96	**99**	**99**	98	96	97	**99**	4
				-	96	96	96	98	96	96	Jl1-36
					-	98	98	96	97	98	Jl1-4
						-	**99**	96	97	**99**	Jl1-1
							-	96	97	**99**	Ag31-3
								-	96	96	Ag31-6
									-	97	Ag31-13
										-	O2-1

Table S5. *In silico* detected mismatches (underlined) of phylotypes Se3-204 and D1-695 with primers and probe EUB338 (I-III) used in this study with.

Primer/Probe	Primer sequence/Probe binding site	
ITSF	5'-GTCGTAACAAGGTAGCCGTA-3'	
Se3-204	5'-GTCGTAACAAGGTA<u>T</u>C<u>TC</u>TA-3'	3 mismatches
D1-695	5'-GTCGTAACAAGGTA<u>T</u>C<u>AC</u>TA-3'	3 mismatches
GM5_341f	5'-CCTACGGGAGGCAGCAG-3'	
Se3-204	5'-<u>T</u>CTACGG<u>A</u>AGGC<u>T</u>GCAG-3'	3 mismatches
EUB338 (I-III)	5'-ACWCCTACGGGWGGCWGC-3'	
Se3-204	5'-ACT<u>T</u>CTACGG<u>A</u>AGGCTGC-3'	2 mismatches

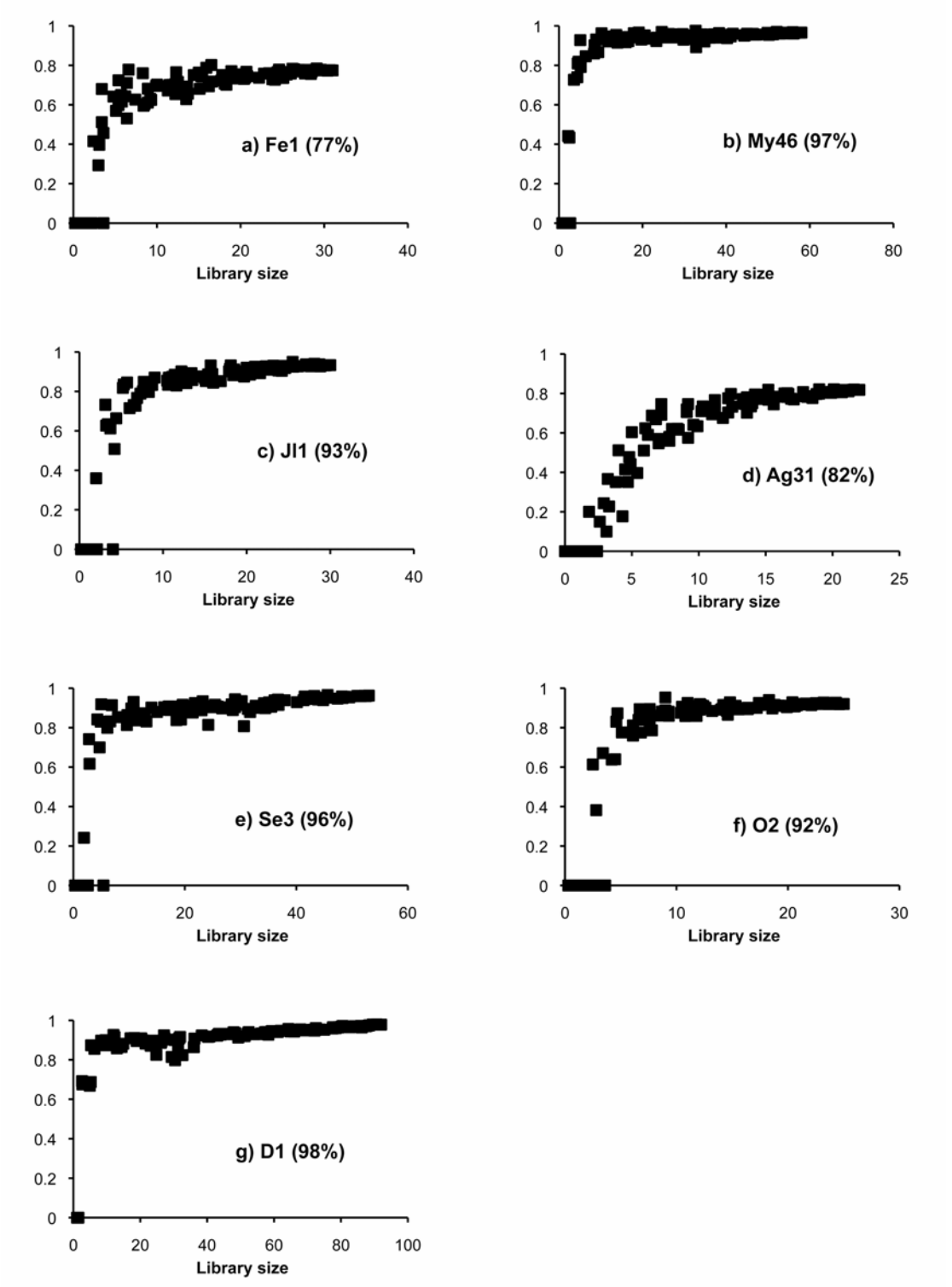

Figure S1. Clone library coverage based on Good's C estimator. The coverage value is indicated for each sample in parenthesis.

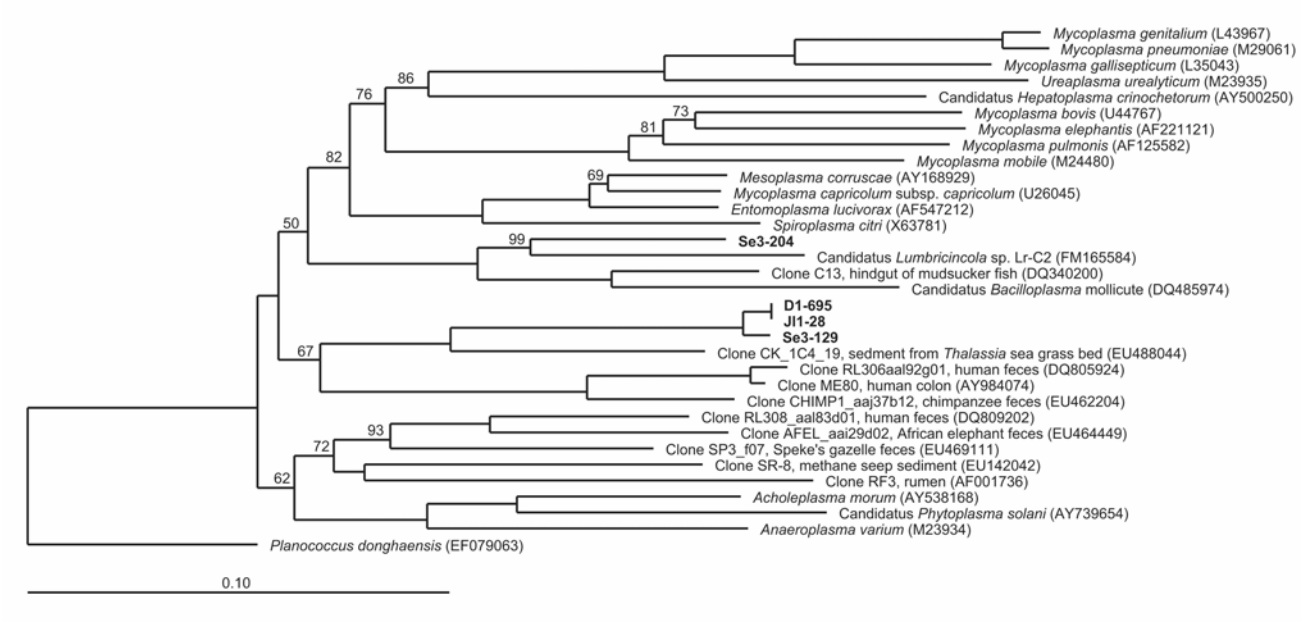

Figure S2. Neighbour-joining tree based on the Mollicutes 16S rRNA sequences from the midgut of *Nephrops norvegicus*. *Planococcus donghaensis* (Firmicutes) was used as an outgroup. The bar corresponds to 10% nucleotide difference and bootstrap values were calculated from 1000 replicate trees. Only bootstrap values over 50% are shown in the tree.

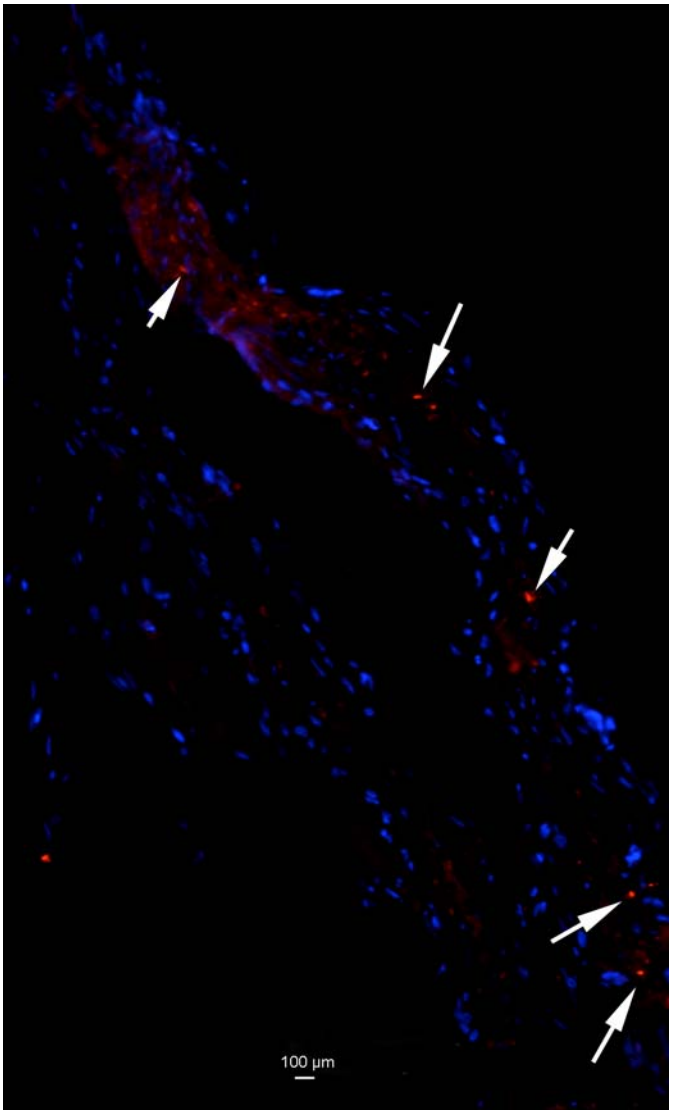

Figure S3. Gut section (thickness 4 µm) of *Nephrops norvegicus* sample FSE3 (September) hybridized with Cy3 labeled probe UncMol89 specific for uncultured Mollicutes phylotype Se3-204 detected in this study. Arrows indicate sarcina-like aggregates of Mollicutes. Blue signal corresponds to DAPI signal from the gut wall epithelial cells and red signal to the hybridized bacteria